

PAPER

Improvement of Detection Performance in DWT-Based Image Watermarking under Specified False Positive Probability

Masayoshi NAKAMOTO^{†a)}, *Member*, Kohei SAYAMA[†], *Student Member*, Mitsuji MUNEYASU^{††}, *Senior Member*, Tomotaka HARANO[†], *Nonmember*, and Shuichi OHNO[†], *Member*

SUMMARY For copyright protection, a watermark signal is embedded in host images with a secret key, and a correlation is applied to judge the presence of watermark signal in the watermark detection. This paper treats a discrete wavelet transform (DWT)-based image watermarking method under specified false positive probability. We propose a new watermarking method to improve the detection performance by using not only positive correlation but also negative correlation. Also we present a statistical analysis for the detection performance with taking into account the false positive probability and prove the effectiveness of the proposed method. By using some experimental results, we verify the statistical analysis and show this method serves to improve the robustness against some attacks.

key words: image watermarking, discrete wavelet transform (DWT), false positive probability, analysis of detection performance

1. Introduction

As the Internet has spread rapidly, the illegal copy and distribution of digital contents without the allowance of the copyright owner would be increased more and more. A digital watermarking has been studied for a copyright protection of digital contents [1]–[3]. It can be achieved that a watermark signal is embedded into the digital contents by using a secret key. After that, the copyright owner can detect the watermark signal by using the secret key in the case of the assertion of the copyright.

The watermark in the digital contents should be robust against common image processing or attacks such as JPEG compression, scaling down, noise addition and cropping. The correlation-based watermark is known as robust method against above image processing or attacks. In this method, the watermark signal is detected based on the correlation between the watermarked coefficients and watermark signal. Cox et al. have proposed a watermarking method in which the pseudo-random number sequence is embedded into the DCT coefficients as a watermark signal, and the watermark signal is detected based on the correlation [4]. Also, Piva et al. have shown the DCT-based watermarking method whose advantage is that the host (uncorrupted original) image is not needed in the detection process [5].

Barni et al. [11] have proposed the DWT-based image watermarking method in which the watermark signal is de-

tected based on the false positive probability which can be calculated by the watermarked DWT coefficients. Though there are many other methods for the DWT-based image watermarking have proposed [6]–[10], the study [11] is especially significant and important because consideration of the false positive rate is useful for judgment of watermark presence. The purpose of this work is to develop a new watermarking method under specified false positive probability and we call the work studied by Barni et al. the conventional method.

For explanation of the conventional method, let the correlation between the watermarked DWT coefficients and watermark signal be ρ . Then it can be expressed as

$$\rho = \rho_{xy} + \rho_w$$

where ρ_{xy} is the correlation between the DWT coefficients of host image and watermark signal, and ρ_w is the watermark element. ρ_{xy} obeys a zero-mean Gaussian distribution. If ρ_{xy} is a negative value, the robustness of the watermark may be decreased. That is, the detection performance is depend on the sign of ρ_{xy} .

The proposed watermarking method is independent of the sign of ρ_{xy} . In the proposed watermarking method, if $\rho_{xy} < 0$, the watermark signal is embedded in negative directions and the absolute correlation is applied in the watermark detection. In this case, the threshold should be changed for the same false positive probability, so we show the statistical analysis for the detection performance based on the new threshold and prove the proposed method is statistically more effective than the conventional method.

Finally, we show the experimental results and verify the statistical analysis. Additionally, we show that this method serves to improve the robustness against JPEG compression, and scaling down and Gaussian noise addition.

2. Conventional Method

2.1 Embedding

As preparatory to the explanation of the proposed method, let us summarize the conventional method proposed in [11].

Consider a host image I whose size is $2M \times 2N$. Decompose I by the DWT, and the embedded area is the subbands $Y_0^0(i, j)$, $Y_0^1(i, j)$ and $Y_0^2(i, j)$ as shown in Fig. 1. The watermark signal is embedded as

Manuscript received August 30, 2010.

[†]The authors are with the Graduate School of Engineering, Hiroshima University, Higashihiroshima-shi, 739-8527 Japan.

^{††}The author is with the Faculty of Engineering Science, Kansai University, Suita-shi, 564-8680 Japan.

a) E-mail: masayoshi@ieec.org

DOI: 10.1587/transfun.E94.A.661

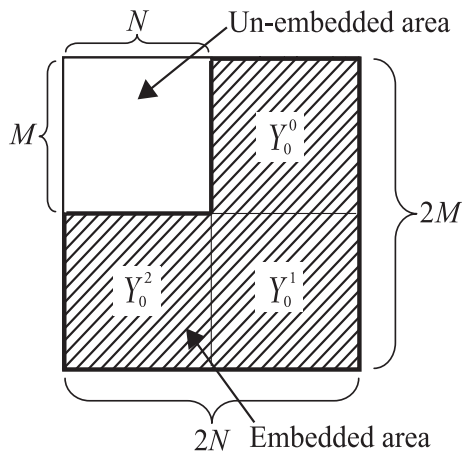


Fig. 1 Embedded area on the DWT domain.

$$\tilde{Y}_0^\theta(i, j) = Y_0^\theta(i, j) + \alpha w^\theta(i, j)x^\theta(i, j) \quad (1)$$

where $w^\theta(i, j)$ is the weighting function and α is the scaling parameter. The watermark signal $x^\theta(i, j)$ is consist of a binary pseudorandom sequence $\{+1, -1\}$. After the watermark signal is embedded in $Y_0^\theta(i, j)$, we can obtain the watermarked images by the inverse DWT (IDWT).

2.2 Detection

We show the detection process of the watermarking method. First, transform the watermarked image to the embedding domain by DWT. Calculate the correlation ρ defined as

$$\rho = \frac{1}{3MN} \sum_{\theta=0}^2 \sum_{i=0}^{M-1} \sum_{j=0}^{N-1} \tilde{Y}_0^\theta(i, j)x^\theta(i, j). \quad (2)$$

Let the threshold be T_ρ , then if

$$\rho > T_\rho, \quad (3)$$

it is judged that the watermark signal is present in the digital image. T_ρ is decided by the false positive probability.

Here the probability density function of ρ is given by

$$p_f(\rho) = \frac{1}{\sqrt{2\pi}\sigma_\rho} \exp\left(-\frac{\rho^2}{2\sigma_\rho^2}\right) \quad (4)$$

where σ_ρ^2 is the variance of ρ which can be expressed as

$$\sigma_\rho^2 = \frac{1}{(3MN)^2} \sum_{\theta=0}^2 \sum_{i=0}^{M-1} \sum_{j=0}^{N-1} E[\{\tilde{Y}_0^\theta(i, j)\}^2]. \quad (5)$$

Since $E[*]$ represents an expected value, in practice, σ_ρ can be calculated as

$$\sigma_\rho^2 \approx \frac{1}{(3MN)^2} \sum_{\theta=0}^2 \sum_{i=0}^{M-1} \sum_{j=0}^{N-1} \{\tilde{Y}_0^\theta(i, j)\}^2. \quad (6)$$

The probability for $\rho \geq T_\rho$ can be expressed as

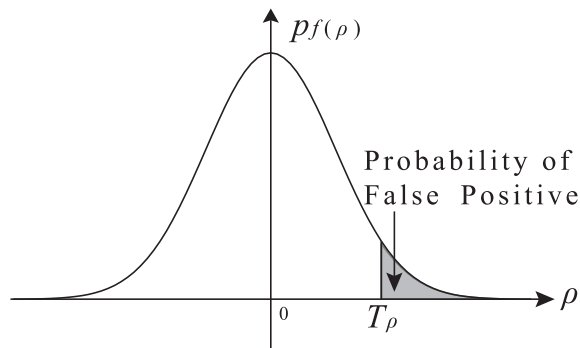


Fig. 2 False positive probability of the one-sided correlation.

$$P_f(\rho \geq T_\rho) = \int_{T_\rho}^{\infty} p_f(\rho) d\rho. \quad (7)$$

This indicates the probability of the false positive as shown in Fig. 2. So we write P_f instead of $P_f(\rho \geq T_\rho)$, and we call P_f the false positive probability. We can calculate the T_ρ by setting P_f . For example, when $P_f = 10^{-8}$, it is calculated as

$$T_\rho = 3.9683 \sqrt{2}\sigma_\rho. \quad (8)$$

2.3 Analysis of Correlation

Assume the key in (2) is the same as the one in the embedding process, we have

$$\rho = \frac{1}{3MN} \sum_{\theta=0}^2 \sum_{i=0}^{M-1} \sum_{j=0}^{N-1} \{Y_0^\theta(i, j)x^\theta(i, j) + \alpha w^\theta(i, j)\}. \quad (9)$$

This can be rewritten as

$$\rho = \rho_{xy} + \rho_w \quad (10)$$

where ρ_{xy} is the correlation of $Y_0^\theta(i, j)$ and $x^\theta(i, j)$ defined as

$$\rho_{xy} = \frac{1}{3MN} \sum_{\theta=0}^2 \sum_{i=0}^{M-1} \sum_{j=0}^{N-1} Y_0^\theta(i, j)x^\theta(i, j) \quad (11)$$

and ρ_w is the element of watermarking signal defined as

$$\rho_w = \frac{\alpha}{3MN} \sum_{\theta=0}^2 \sum_{i=0}^{M-1} \sum_{j=0}^{N-1} w^\theta(i, j). \quad (12)$$

Because $Y_0^\theta(i, j)$ and $x^\theta(i, j)$ is uncorrelated, ρ_{xy} is much smaller than ρ_w in (10), and ρ_{xy} is statistically regarded as 0. Thus, it is obvious that

$$\rho_w \gg \rho_{xy} \approx 0 \quad (13)$$

So if ρ_w (the watermark strength) is large enough, (3) can be satisfied.

Since ρ_{xy} obeys a zero-mean Gaussian distribution, the amplitude of the correlation ρ is depend on ρ_{xy} . That is, the detection performance also depends on the sign of ρ_{xy} , or

the combination of secret key and host image. Especially, if the variance of ρ_{xy} is large, the detection performance vary greatly. In that case, ρ_{xy} has the potential to become a large negative and the detection performance may degrade seriously.

3. Proposed Method

3.1 Embedding

We propose a new watermarking method in which the detection performance is not degraded when $\rho_{xy} < 0$.

First, we show an embedding algorithm. Before embedding the watermark signal, decompose the host image by the DWT, and calculate ρ_{xy} using $Y_0^\theta(i, j)$ and $x^\theta(i, j)$ based on (11). After calculating ρ_{xy} , the watermark signal is embedded according to ρ_{xy} as

$$\tilde{Y}_0(i, j) = \begin{cases} Y_0^\theta(i, j) + \alpha w^\theta(i, j)x^\theta(i, j), & \rho_{xy} > 0 \\ Y_0^\theta(i, j) - \alpha w^\theta(i, j)x^\theta(i, j), & \rho_{xy} < 0. \end{cases} \quad (14)$$

That is, we decide the direction of watermark signal based on the sign of ρ_{xy} .

3.2 Detection

The detection rule of watermark should be also changed. It is judged that the watermark signal is present in the image if

$$\rho < -T_{|\rho|} \text{ or } \rho > T_{|\rho|} \quad (15)$$

where $T_{|\rho|}$ is a new threshold defined as shown in Fig. 3. (15) is equivalent to

$$|\rho| > T_{|\rho|}. \quad (16)$$

If the keys using embedding process and detection process (or $x^\theta(i, j)$ in (14) and (2)) are the same, we have

$$\rho = \begin{cases} \rho_{xy} + \rho_w, & \rho_{xy} > 0 \\ \rho_{xy} - \rho_w, & \rho_{xy} < 0 \end{cases} \quad (17)$$

by substituting (14) into (2).

It follows from (17) that the absolute correlation can expressed as

$$|\rho| = |\rho_{xy}| + \rho_w. \quad (18)$$

From (18), we can see that the amplitude of $|\rho|$ does not depended on the sign of ρ_{xy} . Thus, the watermark signal is detected based on (16) by calculating

$$|\rho| = \frac{1}{3MN} \left| \sum_{\theta=0}^2 \sum_{i=0}^{M-1} \sum_{j=0}^{N-1} \tilde{Y}_0^\theta(i, j)x^\theta(i, j) \right|. \quad (19)$$

Next, we show the decision of the new threshold $T_{|\rho|}$

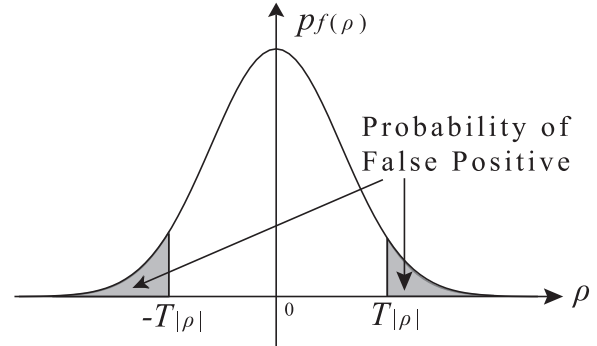


Fig. 3 False positive probability of the dual-sided correlation.

when using the new detection rule. The probability density function of ρ is given by (4). Hence it follows from Fig. 3 that the false positive probability is

$$\begin{aligned} P_f(\rho \leq -T_{|\rho|}, \rho \geq T_{|\rho|}) &= \int_{-\infty}^{-T_{|\rho|}} p_f(\rho) d\rho + \int_{T_{|\rho|}}^{\infty} p_f(\rho) d\rho \\ &= 2 \int_{T_{|\rho|}}^{\infty} p_f(\rho) d\rho. \end{aligned} \quad (20)$$

From (20), the new threshold $T_{|\rho|}$ can be calculated by giving the false positive probability P_f . For example, if P_f is given as 10^{-8} , it can be calculated as

$$T_{|\rho|} = 4.0522 \sqrt{2} \sigma_\rho. \quad (21)$$

From Figs. 2 and 3, it is obvious that

$$T_{|\rho|} > T_\rho, \quad (22)$$

under the same false positive probability.

Here, let the increment of correlation be $\Delta\rho$ defined as

$$\Delta\rho = |\rho| - \rho. \quad (23)$$

Then we have

$$\Delta\rho = \begin{cases} 0, & \rho_{xy} > 0, \text{ (Probability is 0.5)} \\ 2|\rho_{xy}|, & \rho_{xy} < 0, \text{ (Probability is 0.5)}. \end{cases} \quad (24)$$

$\Delta\rho$ takes two values as (24) with same probability (0.5). When $\rho_{xy} > 0$, (22) and (24) imply that the detection performance of the proposed method is approximately the same (slightly degraded) because there is not much difference between $T_{|\rho|}$ and T_ρ . On the other hand, when $\rho_{xy} < 0$, the detection performance of the proposed method is improved if

$$\Delta\rho = 2|\rho_{xy}| > T_{|\rho|} - T_\rho. \quad (25)$$

The sign of ρ_{xy} is positive or negative with the same probability (0.5), so we show the effectiveness of the proposed method by statistical analysis in the next section.

4. Statistical Analysis for the Detection Performance

From (24), we can see that $\Delta\rho$ is a stochastic variable. So let us analyze the detection performance based on statistics, and compare the proposed method with conventional method [11] under the same false positive probability.

First, let the variance of ρ_{xy} be σ_{xy}^2 and the variance of the watermark signal be σ_w^2 as

$$\sigma_{xy}^2 = \frac{1}{(3MN)^2} \sum_{\theta=0}^2 \sum_{i=0}^{M-1} \sum_{j=0}^{N-1} \{Y_0^\theta(i, j)\}^2 \tag{26}$$

$$\sigma_w^2 = \frac{1}{(3MN)^2} \sum_{\theta=0}^2 \sum_{i=0}^{M-1} \sum_{j=0}^{N-1} \{\alpha w^\theta(i, j)\}^2, \tag{27}$$

respectively. According to the property of variance, σ_ρ^2 can be

$$\sigma_\rho^2 = \sigma_{xy}^2 + \sigma_w^2 \tag{28}$$

where σ_ρ^2 is expressed by (6).

Substituting (10) and (18) into (23), we have

$$\Delta\rho = |\rho_{xy}| - \rho_{xy}. \tag{29}$$

According to (24), $\Delta\rho$ is decided based on the sign of ρ_{xy} . Since ρ_{xy} obeys a Gaussian distribution with zero mean, we consider the statistical value $E[\Delta\rho]$ as

$$E[\Delta\rho] = E[|\rho_{xy}|] - E[\rho_{xy}]. \tag{30}$$

The expected value of ρ_{xy} is calculated as

$$\begin{aligned} E[\rho_{xy}] &= \frac{1}{\sqrt{2\pi}\sigma_{xy}} \int_{-\infty}^{\infty} \rho \exp\left(-\frac{\rho^2}{2\sigma_{xy}^2}\right) d\rho \\ &= 0. \end{aligned} \tag{31}$$

Whereas, the expected value of $|\rho_{xy}|$ is

$$\begin{aligned} E[|\rho_{xy}|] &= \frac{1}{\sqrt{2\pi}\sigma_{xy}} \int_0^{\infty} 2\rho \exp\left(-\frac{\rho^2}{2\sigma_{xy}^2}\right) d\rho \\ &= \frac{2\sigma_{xy}}{\sqrt{2\pi}}. \end{aligned} \tag{32}$$

From (31) and (32), we have

$$E[\Delta\rho] = E[|\rho_{xy}|] = \frac{2\sigma_{xy}}{\sqrt{2\pi}}. \tag{33}$$

In order to compare with $E[\Delta\rho]$, let us consider the increment of threshold defined as

$$\Delta T_\rho = T_{|\rho|} - T_\rho. \tag{34}$$

Then, considering (8), (21) and (34), we have

$$\Delta T_\rho = \sqrt{2}\gamma\sigma_\rho \tag{35}$$

Table 1 Relationship between the parameters P_f , γ , T_ρ and $T_{|\rho|}$.

P_f	γ	T_ρ	$T_{ \rho }$
10^{-8}	0.0839	$3.9683 \sqrt{2}\sigma_\rho$	$4.0522 \sqrt{2}\sigma_\rho$
10^{-7}	0.0901	$3.6765 \sqrt{2}\sigma_\rho$	$3.7666 \sqrt{2}\sigma_\rho$
10^{-6}	0.0977	$3.3612 \sqrt{2}\sigma_\rho$	$3.4589 \sqrt{2}\sigma_\rho$
10^{-5}	0.1077	$3.0157 \sqrt{2}\sigma_\rho$	$3.1234 \sqrt{2}\sigma_\rho$
10^{-4}	0.1213	$2.6297 \sqrt{2}\sigma_\rho$	$2.7510 \sqrt{2}\sigma_\rho$
10^{-3}	0.1417	$2.1851 \sqrt{2}\sigma_\rho$	$2.3268 \sqrt{2}\sigma_\rho$
10^{-2}	0.1764	$1.6450 \sqrt{2}\sigma_\rho$	$1.8214 \sqrt{2}\sigma_\rho$
10^{-1}	0.2569	$0.9062 \sqrt{2}\sigma_\rho$	$1.1631 \sqrt{2}\sigma_\rho$

where γ is the parameter calculated by the false positive probability. For example, when the false positive probability is 10^{-8} , it follows from (8) and (21) that

$$\begin{aligned} \gamma &\approx 4.0522 - 3.9783 \\ &= 0.0839. \end{aligned} \tag{36}$$

Table 1 shows the relationship between the parameters γ , T_ρ and $T_{|\rho|}$ in the case from $P_f = 10^{-8}$ to $P_f = 10^{-1}$. From Table 1, we can see that the difference of threshold expands as the false positive probability rises.

Next, for discussion of superiority of the proposed method, define the difference between $E[|\rho_{xy}|]$ and ΔT_ρ as

$$\delta = E[\Delta\rho] - \Delta T_\rho. \tag{37}$$

δ indicates a performance index and is very important parameter in this paper. If $\delta > 0$, the increment of correlation is statistically larger than that of threshold and it is concluded that the use of the absolute correlation is more effective than the case of using just the positive correlation (conventional method) for the watermark detection.

Here, let us consider and analyze the sign of δ . Substituting (33) and (35) into (37) yields

$$\delta = \frac{2\sigma_{xy}}{\sqrt{2\pi}} - \gamma \sqrt{2\sigma_{xy}^2 + 2\sigma_w^2}. \tag{38}$$

Consequently, δ becomes small as γ (P_f) or σ_w takes the large value.

Let us consider a practical upper bound for the false positive probability and σ_w^2 in the watermark application. Taking into account the image quality, it is appropriate that the element of watermark signal is always smaller than that of the DWT coefficients of the host image. So it is clear that the relationship

$$\sigma_{xy}^2 > \sigma_w^2 \tag{39}$$

is hold. In the case when (39) is not satisfied, the image quality should be considerably degraded. It follows from (39) that (38) is

$$\delta > \frac{2\sigma_{xy}}{\sqrt{2\pi}} - 2\gamma\sigma_{xy}. \tag{40}$$

Next, let us consider the upper bound of γ . Usually it is desirable that the false positive probability is as small as

possible. However, as we can see from Table 1, if you set the false positive probability is too small, the threshold raises and it leads to the increase of false negative. The purpose of this work is to estimate the lower bound of δ , we just consider the upper bound of the false positive probability. The false positive probability is decided by user, however, it is practically enough that the upper bound of the probability is 10^{-1} , that is

$$P_f \leq 10^{-1}. \tag{41}$$

For example, in [11], the threshold is calculated by setting the false positive probability to be 10^{-8} . Also, the detection results with 1000 different pseudo random number sequences are shown in [6] and it implies that the false positive probability is smaller than 10^{-3} . From above facts, we think (41) is an appropriate condition in the watermark detection.

According to the case of the false positive probability 10^{-1} in Table 1, we have

$$\gamma < 0.2569. \tag{42}$$

From (40) and (42), we have

$$\delta > 0.2841\sigma_{xy} > 0. \tag{43}$$

Based on the above analysis and result (43), it can be concluded that

$$E[\Delta\rho] > \Delta T_\rho \tag{44}$$

is valid under two conditions (39) and (41).

This implies that the threshold of the proposed method raises and therefore the detection performance is degraded when $\rho_{xy} > 0$, however, the detection performance is dramatically improved when $\rho_{xy} < 0$. By verifying the effectiveness of these detection methods statistically, we conclude that the proposed method is superior to the conventional method [11] under the same false positive probability.

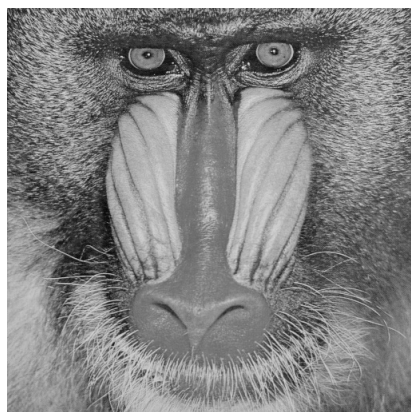
5. Experimental Results

5.1 Statistical Evaluation

Let us use two host images Bridge and Mandrill (Fig. 4) whose sizes are both $M = N = 512$. $w(i, j)$ are decided based on the human visual system (HVS) [12] as well as [11], where α is calculated with PSNR = 30 [dB] and PSNR = 50 [dB] according to Appendix. Figures 5 and 6 show the watermarked images Bridge and Mandrill by using the proposed method in the case of PSNR = 30 [dB] and



(a) Bridge

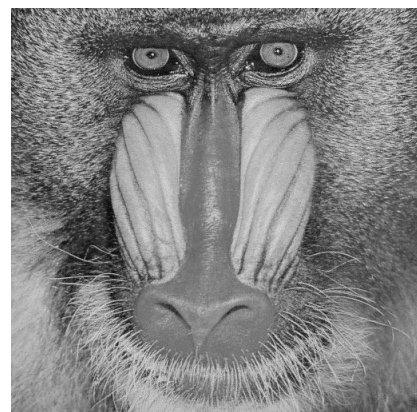


(b) Mandrill

Fig. 4 Host images.



(a) Bridge



(b) Mandrill

Fig. 5 Watermarked images (PSNR = 30 dB).

Table 2 Calculation results of σ_{xy} , $E[|\rho_{xy}|]$ and the experimental results of expected value of $|\rho_{xy}|$.

Image	σ_{xy}^2	$E[\rho_{xy}]$	$\frac{1}{10000} \sum_{i=1}^{10000} \rho_{xy}^{(i)} $
Bridge	0.001193	0.0276	0.0277
Mandrill	0.002005	0.0360	0.0357

Table 3 Calculation results of σ_w^2 and σ_ρ^2 .

Image	PSNR	σ_w^2	σ_ρ^2
Bridge	50	4.4098×10^{-6}	0.001197
	30	4.4098×10^{-4}	0.001638
Mandrill	50	4.4098×10^{-6}	0.002009
	30	4.4098×10^{-4}	0.002452

Table 4 Calculation results of thresholds, its increment ΔT_ρ and δ .

(a) PSNR = 30 dB

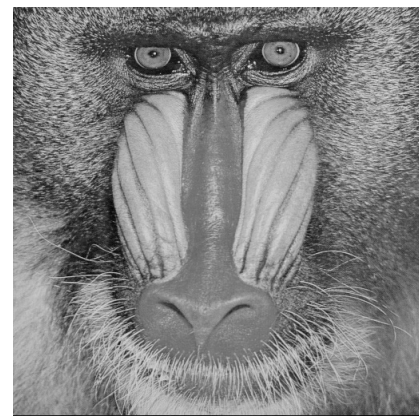
Image	P_f	T_ρ	$T_{ \rho }$	ΔT_ρ	δ
Bridge	10^{-8}	0.2271	0.2319	0.0048	0.0228
	10^{-7}	0.2104	0.2156	0.0052	0.0224
	10^{-6}	0.1924	0.1980	0.0056	0.0220
	10^{-5}	0.1726	0.1788	0.0062	0.0214
	10^{-4}	0.1505	0.1575	0.0069	0.0207
	10^{-3}	0.1251	0.1332	0.0081	0.0195
	10^{-2}	0.0942	0.1043	0.0101	0.0175
	10^{-1}	0.0519	0.0666	0.0147	0.0129
Mandrill	10^{-8}	0.2779	0.2838	0.0059	0.0301
	10^{-7}	0.2575	0.2638	0.2638	0.0297
	10^{-6}	0.2354	0.2422	0.0068	0.0292
	10^{-5}	0.2112	0.2187	0.0075	0.0285
	10^{-4}	0.1842	0.1926	0.0085	0.0275
	10^{-3}	0.1530	0.1629	0.0099	0.0261
	10^{-2}	0.1152	0.1276	0.0124	0.0236
	10^{-1}	0.0635	0.0815	0.0180	0.0180

(b) PSNR = 50 dB

Image	P_f	T_ρ	$T_{ \rho }$	ΔT_ρ	δ
Bridge	10^{-8}	0.1941	0.1983	0.0041	0.0235
	10^{-7}	0.1799	0.1843	0.0044	0.0232
	10^{-6}	0.1645	0.1692	0.0048	0.0228
	10^{-5}	0.1476	0.1528	0.0053	0.0223
	10^{-4}	0.1287	0.1346	0.0059	0.0217
	10^{-3}	0.1069	0.1138	0.0069	0.0207
	10^{-2}	0.0805	0.0891	0.0086	0.0190
	10^{-1}	0.0443	0.0569	0.0126	0.0150
Mandrill	10^{-8}	0.2515	0.2569	0.0053	0.0307
	10^{-7}	0.2330	0.2388	0.0057	0.0303
	10^{-6}	0.2131	0.2193	0.0062	0.0298
	10^{-5}	0.1912	0.1980	0.0068	0.0292
	10^{-4}	0.1667	0.1744	0.0077	0.0283
	10^{-3}	0.1385	0.1475	0.0090	0.0270
	10^{-2}	0.1043	0.1155	0.0112	0.0248
	10^{-1}	0.0574	0.0737	0.0163	0.0197



(a) Bridge



(b) Mandrill

Fig. 6 Watermarked images (PSNR = 50 dB).

PSNR = 50 [dB]. Generally, it is considered that the lower bound of PSNR is approximately 40 [dB] from the image quality point of view. However, since the embedding algorithm is based on the HVS, we set the lower bound of PSNR is 30 [dB] in this paper.

As mentioned in the foregoing section, ρ_{xy} is decided by the combination of the watermark signal (secret key) and host image, that is, the detection performance is depend on ρ_{xy} . Since ρ_{xy} obeys the Gaussian distribution $N(0, \sigma_{xy})$, the statistical analysis is needed to compare the effectiveness of two methods.

First, we transform the host images into the DWT domain and calculate σ_{xy} and $E[|\rho_{xy}|]$ which is obtained by (33). Table 2 shows the calculation results of σ_{xy} , $E[|\rho_{xy}|]$ and the experimental results of expected value of $|\rho_{xy}|$ which is calculated as

$$\frac{1}{10000} \sum_{i=1}^{10000} |\rho_{xy}^{(i)}|, \tag{45}$$

where the 10000 correlations $\rho_{xy}^{(1)}, \rho_{xy}^{(2)} \dots \rho_{xy}^{(10000)}$ are calculated by the 10000 different watermark signals. We can see that $E[|\rho_{xy}|]$ are approximately consistent with the experimental results of expected value of $|\rho_{xy}|$, that is, (33) is confirmed experimentally.



Fig. 7 1/2 scale image of Bridge.

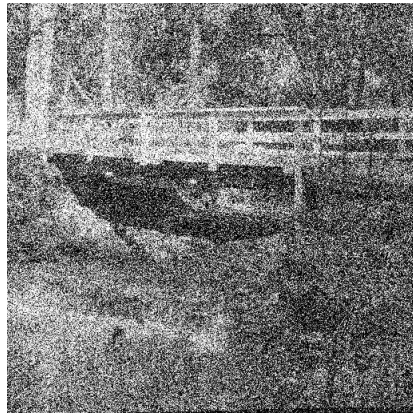


Fig. 8 Noised image of Bridge.

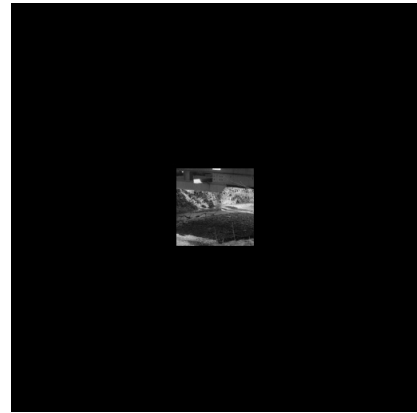


Fig. 9 Cropped image of Bridge.

Table 3 shows the calculation results of σ_w and σ_ρ in the case of PSNR = 30 [dB] and PSNR = 50 [dB]. Also, Table 4 shows the threshold values, the increment value of the threshold and the performance index δ where T_ρ and $T_{|\rho|}$ are both calculated with $P_f = 10^{-8}$ – 10^{-1} . From Tables 2 and 3, we can see that (39) is satisfied even when the quality of watermarked images are PSNR = 30 dB.

From Table 4, we can see

$$\delta > 0$$

and it is confirmed that the proposed method statistically outperforms the conventional method under the conditions:

$$P_f \leq 10^{-1} \tag{46}$$

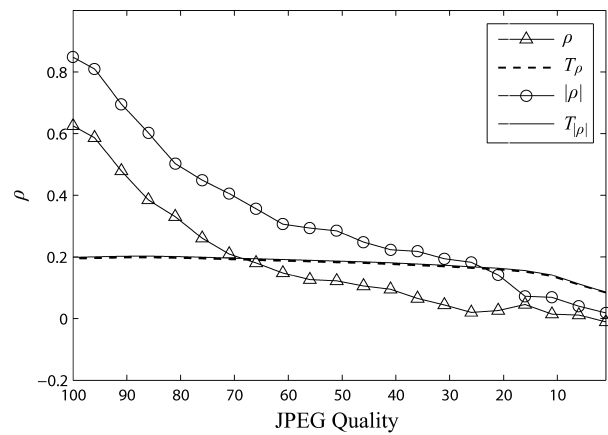
and

$$\text{PSNR} \geq 30 \text{ [dB]}. \tag{47}$$

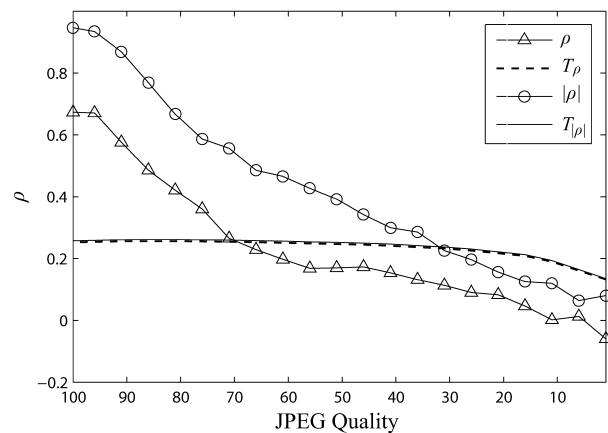
From Tables 2 and 3, (39) is satisfied when (47) is hold. Hence the statistical analysis is verified by the experimental results.

5.2 Robustness against Some Attacks

Let us consider the robustness after attacking. We use two watermarked images as shown in Fig. 6 with PSNR = 50 [dB] and set $P_f = 10^{-8}$ assuming an ordinary situation. As discussed before, when the variance of ρ_{xy} is large and ρ_{xy} is large negative, ρ is smaller and the robustness of the watermark also decreases. In such a situation, we think the proposed method is especially effective. So we treat here the



(a) Bridge



(b) Mandrill

Fig. 10 Comparison of robustness against JPEG compression.

case when ρ_{xy} is large negative.

Figures 10 and 11 show the watermark robustnesses against JPEG compression and scaling down (see Fig. 7), respectively. Since JPEG compression and scaling down are same kind attacking in that just high frequency elements are deleted, and most information of ρ_{xy} can be retained. Against such a low-pass filtering attacks, we think that the

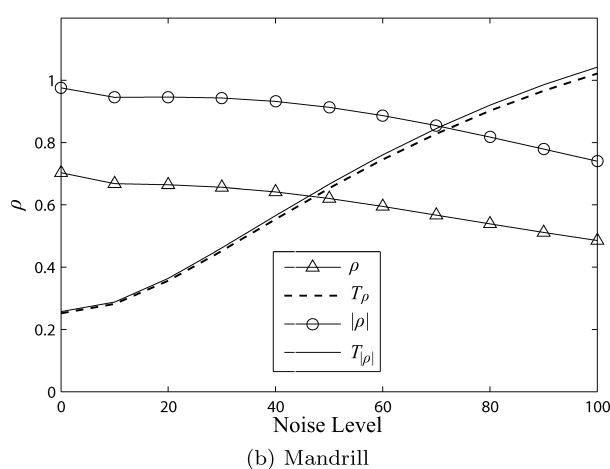
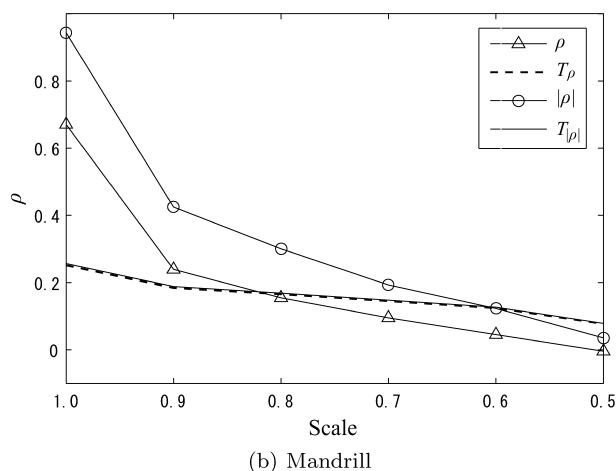
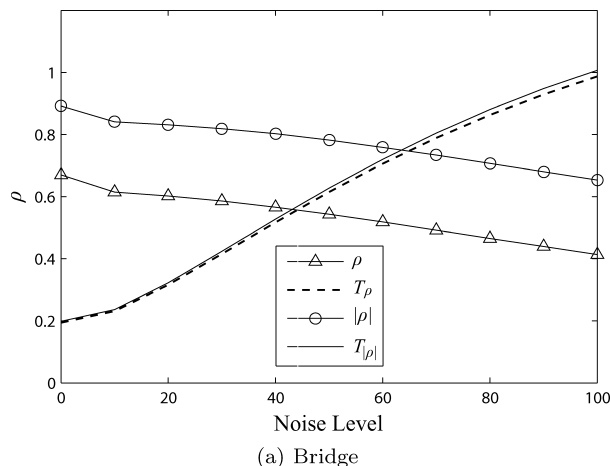
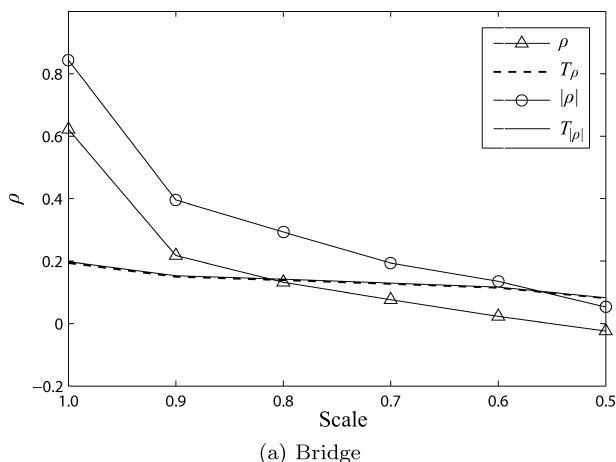


Fig. 11 Comparison of robustness against scaling down.

Fig. 12 Comparison of robustness against Gaussian noise addition.

detection performance of the proposed method can be improved and it can be confirmed from Figs. 10 and 11.

Figure 12 show the watermark robustnesses against Gaussian noise addition (see Fig. 8) where the ρ and $|\rho|$ are the average of 30 results. After Gaussian noise addition, $\Delta\rho$ is expressed as

$$\Delta\rho = 2|\rho_{xy}| - \frac{2}{3MN} \sum_{\theta=0}^2 \sum_{i=0}^{M-1} \sum_{j=0}^{N-1} x^\theta(i, j)U^\theta(i, j) \quad (48)$$

where $U^\theta(i, j)$ are a noise elements in the DWT domain. The second term of (48) is statistically zero, so $\Delta\rho$ is almost constant if we use the average of some results. Also, the variance is

$$\sigma_\rho^2 = \sigma_y^2 + \sigma_w^2 + \sigma_U^2 \quad (49)$$

where σ_U^2 indicates the variance of Gaussian noise in the DWT domain. That is, the variances become larger and it follows that the thresholds are also larger. From Fig. 12, we can verify the above conjecture.

Finally, Fig.13 show the watermark robustnesses against cropping (see Fig. 9) in the watermark detection by using the proposed method and conventional method. When

the cropped size is small, there is no discernible difference in both methods because not only the high frequency elements but also low frequency elements of ρ_{xy} are lost by cropping attacking.

On the other hand, if $\rho_{xy} \geq 0$, the difference of threshold values is corresponding to the detection performance because the correlations ρ and $|\rho|$ are exactly same. From Figs. 10–13, we can see that the difference of threshold values is very slight, so we think the detection performance of the two methods are almost same when $\rho_{xy} \geq 0$.

From simulation results, we can see that the proposed method is particularly useful against low-pass filtering attacks (JPEG compression attack, scaling down) and Gaussian noise addition. Also we confirm the proposed method is much useful to improve the watermark robustness when the variance of correlation is large and ρ_{xy} is large negative.

6. Conclusion

We have proposed the DWT-Based Image watermarking method under specified false positive probability. We compare the detection performance of proposed method and conventional method [11] with same false positive probability, and show the proposed method is statistically more

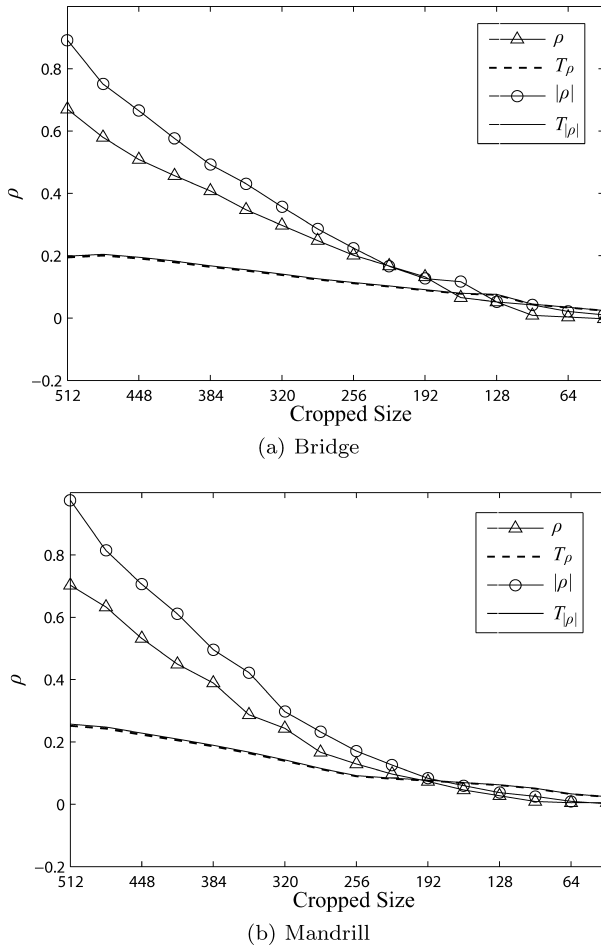


Fig. 13 Comparison of robustness against cropping.

effective than the conventional method. From simulation results, we verify the statistical analysis, and show the proposed method is more robust than the conventional method against JPEG compression, scaling down and Gaussian noise addition attacks.

References

- [1] A. Miyazaki, "Digital watermarking for images—Its analysis and improvement using digital signal processing technique," *IEICE Trans. Fundamentals*, vol.E85-A, no.3, pp.582–590, March 2002.
- [2] M. Barni and F. Bartolini, "Watermarking systems engineering," *Signal Processing and Communications Series*, Marcel Dekker, Feb. 2004.
- [3] I.J. Cox, M.L. Miller, J.A. Bloom, J. Fridrich, and T. Kalker, *Digital watermarking and steganography*, second ed., Morgan Kaufmann Series in Multimedia Information and Systems, Morgan Kaufmann, Nov. 2007.
- [4] I.J. Cox, J. Killian, T. Leighton, and T. Shamoan, "Secure spread spectrum watermark for multimedia," *IEEE Trans. Image Process.*, vol.6, no.12, pp.1673–1687, Dec. 1997.
- [5] A. Piva, M. Barni, F. Bartolini, and V. Cappellini, "DCT-based watermark recovering without resorting to the uncorrupted original image," *Proc. IEEE Int. Conf. Image Process.*, vol.1, pp.520–523, Oct. 1997.
- [6] A. Miyazaki and O. Kabashima, "Improvement of perceptual watermarking based on the multiresolution analysis of still images,"

IEICE Trans. Fundamentals (Japanese Edition), vol.J85-A, no.1, pp.103–111, Jan. 2002.

- [7] M. Ejima and A. Miyazaki, "An analysis of correlation-based watermarking systems," *IEICE Trans. Fundamentals (Japanese Edition)*, vol.J85-A, no.11, pp.1273–1283, Nov. 2002.
- [8] M. Tsai and C. Shen, "Differential energy based watermarking algorithm using Wavelet Tree Group Modulation (WTGM) and human visual system," *IEICE Trans. Fundamentals*, vol.E91-A, no.8, pp.1961–1973, Aug. 2008.
- [9] G. Wu and P. Huang, "A novel entropy based image watermarking in wavelet domain," *IEICE Trans. Fundamentals*, vol.E91-B, no.10, pp.3313–3325, Oct. 2008.
- [10] K. Liu, "Just noticeable distortion model and its application in color image watermarking," *IEICE Trans. Fundamentals*, vol.E92-A, no.2, pp.563–576, Feb. 2009.
- [11] M. Barni, F. Bartolini, and I.A. Piva, "Improved wavelet-based watermarking through pixel-wise masking," *IEEE Trans. Image Process.*, vol.10, no.5, pp.783–791, May 2001.
- [12] A.S. Lewis and G. Knowles, "Image compression using the 2-D wavelet transform," *IEEE Trans. Image Process.*, vol.1, no.2, pp.244–250, April 1992.

Appendix: Calculation of α under Specified PSNR

PSNR is defined as

$$\text{PSNR} = 10 \log_{10} \frac{\sum_{i=0}^{2M-1} \sum_{j=0}^{2N-1} A^2}{\sum_{i=0}^{2M-1} \sum_{j=0}^{2N-1} \{g(i, j) - \tilde{g}(i, j)\}^2} \quad (\text{A} \cdot 1)$$

where $g(i, j)$ is the luminance of original image, $\tilde{g}(i, j)$ is the luminance of watermarked image and A is a dynamic range. Here consider the watermarked elements in the DWT domain with $\alpha = 1$ as

$$E_w(i, j) = w(i, j)x(i, j). \quad (\text{A} \cdot 2)$$

Let the IDWT of (A·2) be $W(i, j)$, then (A·1) can be rewritten as

$$\text{PSNR} \approx 10 \log_{10} \frac{\sum_{i=0}^{2M-1} \sum_{j=0}^{2N-1} A^2}{\alpha^2 \sum_{i=0}^{2M-1} \sum_{j=0}^{2N-1} \{W(i, j)\}^2}. \quad (\text{A} \cdot 3)$$

Hence α is obtained as

$$\alpha \approx \left\{ \frac{10^{-\frac{\text{PSNR}}{10}} \sum_{i=0}^{2M-1} \sum_{j=0}^{2N-1} A^2}{\sum_{i=0}^{2M-1} \sum_{j=0}^{2N-1} \{W(i, j)\}^2} \right\}^{1/2} \quad (\text{A} \cdot 4)$$

by giving specified PSNR.



Masayoshi Nakamoto received the B.E. and M.E. degrees from Okayama University of Science, Okayama, Japan, in 1997 and 1999, respectively, and the Dr.Eng. degree from Hiroshima University, Higashihiroshima, Japan, in 2002. From April 2002 to March 2005, he was JSPS Research fellow. He is currently a research associate of Graduate School of Engineering, Hiroshima University, Higashihiroshima, Japan. His research interests are in the areas of stochastic process, digital signal processing and combinatorial optimization. Dr. Nakamoto is a member of IEEJ and IEEE.

Dr. Nakamoto is a member of IEEJ and IEEE.



Kohei Sayama received the B.E. degree from Hiroshima University, Higashihiroshima, Japan, in 2010. His research interests are in the areas of digital signal processing.



Mitsuji Muneyasu received the B.E. and M.E. degrees in system engineering from Kobe University, in 1982 and 1984, respectively and the Dr.E. degree from Hiroshima University, Japan in 1993. In 1984, he joined Oki Electric Industry Co., Ltd., in Tokyo, Japan. From 1990 to 1991, he was a Research Assistant at the Faculty of Engineering, Tottori University, Tottori, Japan. From 1991 to 2001, he was a Research Assistant and Associate Professor at the Faculty of Engineering, Hiroshima University,

Higashihiroshima, Japan. Since 2001 he joined the Faculty of Engineering, Kansai University, Osaka, Japan, where he is currently a Professor. His research interests include image processing theory and nonlinear digital signal processing. He is a member of IEEE and IPSJ.



Tomotaka Harano received the B.E. and M.E. degree from Hiroshima University, Higashihiroshima, Japan, in 2008 and 2010, respectively. His research interests are in the areas of digital signal processing.



Shuichi Ohno received the B.E., M.E. and Dr.Eng. degrees in applied mathematics and physics from Kyoto University, in 1990, 1992 and 1995, respectively. From 1995 to 1999 he was a research associate in the Department of Mathematics and Computer Science at Shimane University, Shimane, Japan. He joined the Department of Artificial Complex Systems Engineering, Hiroshima University, Hiroshima, Japan, in April 2002, where he is currently an Associate Professor. His current interests are in

the areas of digital communications, signal processing for communications and adaptive signal processing. Dr. Ohno is a member of the IEEE, the Society of Instrument and Control Engineers, and the Institute of Systems, Control, and Information Engineers in Japan.